

Acute or Chronic Upregulation of Mitochondrial Fatty Acid Oxidation Has No Net Effect on Whole-Body Energy Expenditure or Adiposity

Kyle L. Hoehn,^{1,2,7} Nigel Turner,^{1,3,7} Michael M. Swarbrick,¹ Donna Wilks,¹ Elaine Preston,¹ Yuwei Phua,¹ Himani Joshi,¹ Stuart M. Furler,¹ Mark Larance,¹ Bronwyn D. Hegarty,^{1,4} Simon J. Leslie,¹ Russell Pickford,⁵ Andrew J. Hoy,¹ Edward W. Kraegen,^{1,4} David E. James,^{1,6,*} and Gregory J. Cooney^{1,3}

¹Diabetes and Obesity Program, Garvan Institute of Medical Research, 384 Victoria Street, Darlinghurst, NSW, 2010, Australia

²Department of Pharmacology, University of Virginia, Charlottesville, VA, 22908

³St Vincent's Hospital Clinical School

⁴School of Medical Sciences

⁵Bioanalytical Mass Spectrometry Facility

⁶School of Biotechnology and Biomolecular Sciences
University of New South Wales, Sydney, NSW, Australia

⁷These authors contributed equally to this work

*Correspondence: d.james@garvan.org.au

DOI 10.1016/j.cmet.2009.11.008

SUMMARY

Activation of AMP-activated protein kinase (AMPK) is thought to convey many of the beneficial effects of exercise via its inhibitory effect on acetyl-CoA carboxylase 2 (ACC2) and promotion of fatty acid oxidation. Hence, AMPK and ACC have become major drug targets for weight loss and improved insulin action. However, it remains unclear whether or how activation of the fatty acid oxidation pathway without a concomitant increase in energy expenditure could be beneficial. Here, we have used either pharmacological (administration of the AMPK agonist 5' aminoimidazole-4-carboxamide-ribose) or genetic means (mutation of the ACC2 gene in mice) to manipulate fatty acid oxidation to determine whether this is sufficient to promote leanness. Both of these strategies increased whole-body fatty acid oxidation without altering energy expenditure or adiposity. We conclude that negative energy balance is a prerequisite for weight reduction, and increased fatty acid oxidation per se has little, if any, effect to reduce adiposity.

INTRODUCTION

Obesity is linked to a number of metabolic diseases, such as type 2 diabetes (T2D) and cardiovascular disease. Energy imbalance, due to either reduced energy expenditure or increased energy consumption, is the ultimate cause of obesity, with excess nutrients being channeled into lipid depots. Although adipose tissue is an ideal energy store over a certain ideal body weight range, excess lipid is thought to contribute to disease either via modulating the circulating adipokine profile or by directly inducing damage in nonadipose tissues (lipotoxic-

ity). In view of the poor success rate of lifestyle change in managing human obesity, alternate solutions have been sought.

Impaired mitochondrial lipid metabolism has been linked to metabolic disease (Savage et al., 2007). Mitochondria are the major site for fatty acid oxidation (FAO), and defects in this process may contribute to nonoxidative utilization of fatty acids, such as triglyceride storage or conversion to lipotoxic intermediates, both of which may increase adiposity and metabolic disease. A decline in mitochondrial function has been observed both during aging (Petersen et al., 2003) and in individuals with T2D (Kelley et al., 2002), suggesting that increasing FAO may prevent lipid storage and improve metabolism. A major caveat is that, thermodynamically, the only way to achieve net weight loss, assuming that energy intake remains constant, is to increase energy usage or decrease energy efficiency by diverting metabolic energy to heat. Normally, electron transport via the mitochondrial electron transport chain (ETC) is tightly coupled to ATP synthesis, so increased oxidation of nutrients would require increased ATP turnover. In the absence of exercise or other forms of ATP hydrolysis, one way to circumvent an oversupply of fuel substrates is to uncouple the mitochondrial ETC from ATP production. Despite an obvious thermodynamic requirement for increased energy expenditure to promote leanness, it is still widely held that increased muscle mitochondrial FAO per se is sufficient to reduce whole-body adiposity.

AMPK-activated protein kinase (AMPK) regulates mitochondrial FAO by phosphorylating and inhibiting the activity of the mitochondrial enzyme ACC2, leading to reduced malonyl-CoA production. This leads to derepression of CPT1 activity and increased long-chain FA entry into mitochondria. Treatment of rodents with AMPK agonists is associated with leanness (Narkar et al., 2008), and deletion of the ACC2 gene in mice has been reported to result in increased FAO coupled with elevated whole-body energy expenditure (Choi et al., 2007) and a marked reduction in whole-body adiposity (Abu-Elheiga et al., 2001). These studies support the notion that increased flux of FA into mitochondria is sufficient to trigger increased whole-body

energy expenditure and leanness. However, how such manipulations trigger increased energy expenditure remains uncertain.

In the current report, we have re-examined the relationship between increased fatty acid oxidation and reduced adiposity by using both pharmacologic and genetic approaches. Our results do not support the hypothesis that increased fatty acid oxidation causes leanness. Rather, as predicted (Randle et al., 1963), increasing the flux of FA into mitochondria without a concomitant increase in energy demand resulted in a shift in substrate oxidation from glucose and other fuels to FA, with no net change in energy balance.

RESULTS

FAO Is Independent of Energy Expenditure

To assess whether increased FAO is associated with increased energy expenditure, we treated rats with a single dose of the AMPK activator 5' aminoimidazole-4-carboxamide-ribose (AICAR) (250 mg/kg subcutaneous injection). AICAR increased ACC2 phosphorylation, decreased malonyl-CoA levels by 55% within 60 min of injection (Figures 1A and 1B), and increased whole-body FAO, as shown by a drop in the respiratory exchange ratio (RER) (Figure 1C), without any change in energy expenditure (VO_2) in the 10 hr following dosing (Figure 1D). This suggests that there was a reciprocal decrease in the oxidation of other substrates. To test this, we treated isolated EDL muscles with AICAR (2 mM) *ex vivo* in the presence of either ^{14}C -palmitate or ^{14}C -glucose tracers. Consistent with the *in vivo* data, AICAR increased palmitate oxidation (+31%, $p < 0.001$; Figure 1E) at the expense of glucose oxidation (-30%, $p < 0.01$; Figure 1F). This substrate-switching effect of AICAR was due to increased fat oxidation rather than impaired glucose availability or glycolysis because plasma lactate levels were elevated 30 min after AICAR treatment *in vivo* (2.4 ± 0.3 versus 1.5 ± 0.3 mM, AICAR versus control, $p < 0.05$) and in the media after palmitate oxidation (27.5 ± 1.3 versus 23.2 ± 1.6 μ mol lactate released/g EDL, AICAR versus control, $p < 0.05$).

As a control, rats were treated with the mitochondrial uncoupler dinitrophenol (DNP) (30 mg/kg oral administration). DNP increased ACC2 phosphorylation, reduced cellular malonyl-CoA levels by 32% (Figures 1A and 1B), increased FAO to a similar extent as AICAR, and increased VO_2 (Figures 1C and 1D). As predicted, in *ex vivo* experiments, DNP (0.5 mM) caused a significant increase in energy demand and increased the oxidation of both palmitate (+62%, $p < 0.01$; Figure 1G) and glucose (+77%, $p < 0.01$; Figure 1H). We observed similar results in rats fed a high-fat diet (HFD) for 21 days; AICAR and DNP increased FAO, whereas only DNP increased VO_2 (Figures 1I and 1J).

Because activation of AMPK with AICAR did not increase energy expenditure in either chow or HFD rats, it is unlikely that this treatment would result in reduced body weight and/or adiposity. Consistent with this, chronic treatment with AICAR (250 mg/kg subcutaneous injection for 10 days) did not result in any difference in body weight gain, food intake, fat mass, or whole-body VO_2 and RER (Figure S1 available online). As predicted (Winder et al., 2000), chronic AICAR increased the activity of several oxidative enzymes and lipid metabolic enzymes in muscle, consistent with increased muscle mitochondrial biogen-

esis (Figure S2). Though we cannot exclude that longer-term activation of AMPK may drive changes in body composition and energy metabolism via a separate AMPK target, such as SIRT1 and/or PGC-1 α (Canto et al., 2009; Jäger et al., 2007), our studies do not support a major role for AMPK-mediated changes in FAO via ACC inhibition in reduced adiposity. To determine the effect of prolonged FAO on leanness and energy expenditure independently of changes in mitochondrial capacity, we created a mouse model of chronic FAO by deleting the ACC2 gene.

Preservation of Energy Neutrality despite Chronic FAO

We created ACC2-deficient mice on a pure C57BL/6 background. We flanked exon 12 of the ACC2 gene, encoding a critical region of the biotin carboxylase motif, with loxP sites and crossed these mice onto a cre-deleter strain to remove exon 12 and introduce an early stop codon, rendering the ACC2 protein inactive (Figure 2A). Cre was bred out, and the resulting mice were confirmed to be deficient in ACC2 by Southern blot (data not shown), PCR (Figure 2B), and western blotting (Figure 2C). Loss of ACC2 resulted in decreased malonyl-CoA levels in skeletal and cardiac muscle, where ACC2 is the predominant isoform (Figure 2D), and a 57% increase in FAO in isolated soleus muscle (Figure 2E).

The functional consequences of ACC2 deletion on whole-body metabolic parameters were then studied in WT and ACC2 $^{-/-}$ littermates. ACC2 $^{-/-}$ mice had increased ($p < 0.05$) whole-body FAO in the dark (0.87 ± 0.02 versus 0.92 ± 0.01 , ACC2 $^{-/-}$ versus WT) cycle and a trend for increased FAO during the light cycle (0.85 ± 0.01 versus 0.88 ± 0.02 , ACC2 $^{-/-}$ versus WT) (Figure 3A); however, this was not accompanied by a change in energy expenditure (WT light 34.2 ± 0.8 and dark 41.9 ± 1.6 ; KO light 33.6 ± 0.7 and dark 42.2 ± 0.8 ml O_2 /kg/hr/100) (Figure 3B). Despite preferential oxidation of FAs in ACC2 $^{-/-}$ mice compared to WT controls, we observed no difference in body weight (Figure 3C) or adiposity between the two groups (Figures 3D and 3E). Although there was no change in serum lactate between genotypes (data not shown), muscle glycogen stores were elevated, and the utilization of glucose for lipid synthesis was increased in the ACC2 $^{-/-}$ mice, providing evidence that the excess available glucose was being used non-oxidatively (Figures 3F and 3G). Because there was no increase in total TAG accumulation in liver or muscle (Figure 3H), the increased amount of lipid being synthesized was likely being used to support FAO. These data confirm our acute experiments with AICAR in Figure 1 and show that long-term changes in FAO are not linked to significant alterations in energy expenditure and adiposity.

To explore whether the chronic elevation in FAO observed with ACC2 deletion could prevent the metabolic defects induced by an HFD, we challenged WT and ACC2 $^{-/-}$ mice with 36 days of high-fat feeding. During this feeding regime, both genotypes consumed similar quantities of food (Figure 4A), gained a similar amount of body weight (Figure 4B), and exhibited similar fat deposition in three separate adipose depots (Figure 4C). There was also no indication that ACC2 $^{-/-}$ mice were protected from HFD-induced insulin resistance, as they displayed similar glucose and insulin tolerance as WT mice did (Figures 4D and S3), and they had similar rates of glucose disposal into skeletal muscle during the glucose tolerance test (Figure 4E) with similar

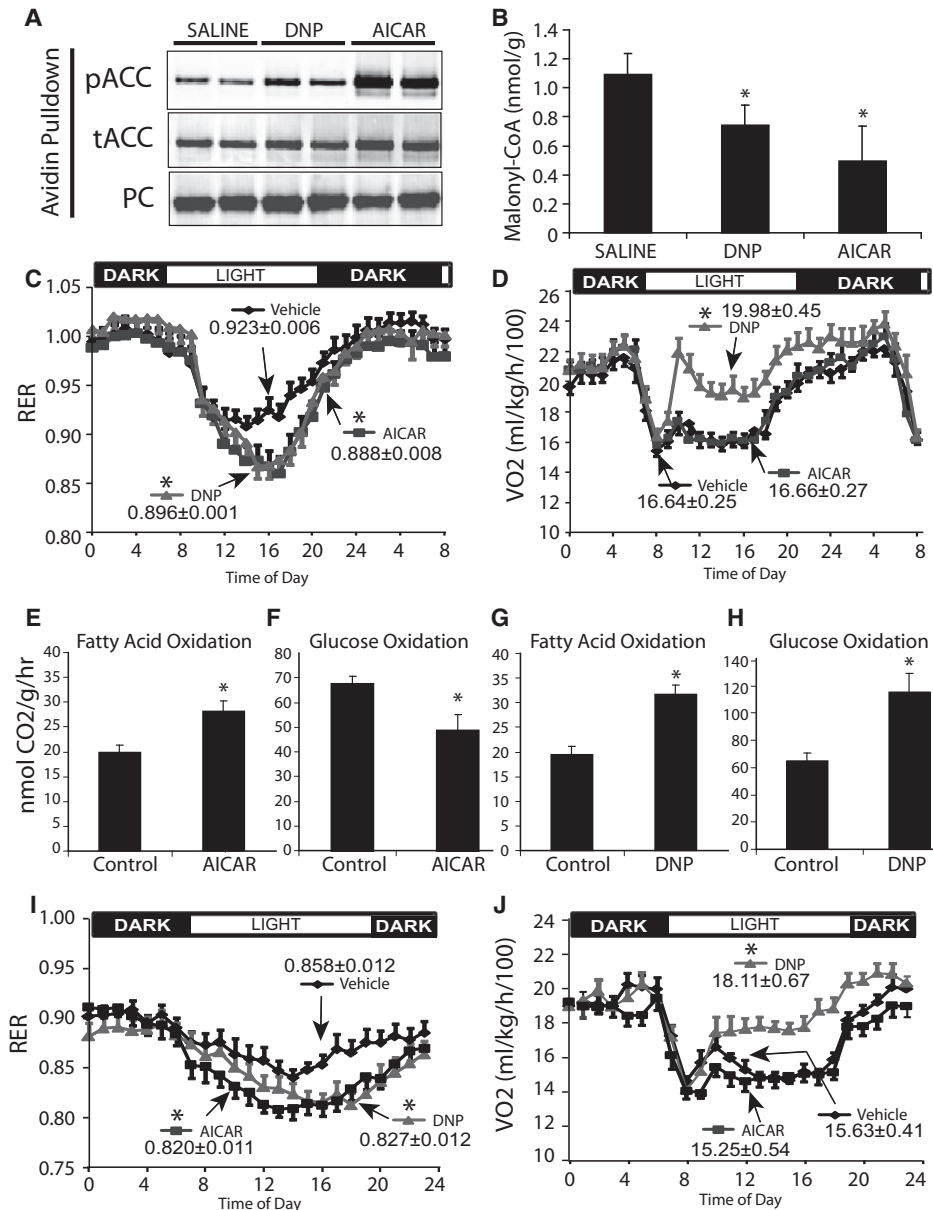


Figure 1. AMPK Activation Drives FAO, but Not Energy Expenditure

Rats were acclimatized overnight and at 10 AM dosed with vehicle (saline), AICAR (250 mg/kg), or DNP (30 mg/kg).

(A) Avidin pulldown from skeletal muscle. ACC phosphorylation and expression 60 min after treatment. Pyruvate carboxylase (PC) is shown as a loading control for the pulldown.

(B) Malonyl-CoA levels in skeletal muscle described in (A).

(C and D) Indirect calorimetry measurement of RER and VO₂ before and after treatment with saline, DNP, or AICAR. Values indicated in the figure represent the average of the 10 hr following dosing.

(E–H) EDL muscle strips were isolated and incubated ex vivo in KHB media with 5 mM glucose and 0.5 mM palmitate and either AICAR (2 mM) or DNP (0.5 mM). Rates of FA and glucose oxidation were measured as described in Experimental Procedures.

(I and J) Indirect calorimetry measurement of RER and VO₂ before and after treatment with saline, DNP, or AICAR in rats fed a high-fat diet for 21 days. Values indicated in the figure represent the average of the 10 hr following dosing.

All results are displayed as means ± SEM. n > 5 and *p < 0.05 for the 10 hr period following dosing.

insulin levels to control mice (Figure 4F). Collectively, these findings suggest that, despite the fact that ACC2^{-/-} mice display increased lipid oxidation, they are not resistant to weight gain or insulin resistance caused by 36 days of an HFD.

DISCUSSION

Body weight and fat mass in mammals are highly robust parameters. Fat mass is very well defended, rendering many lifestyle

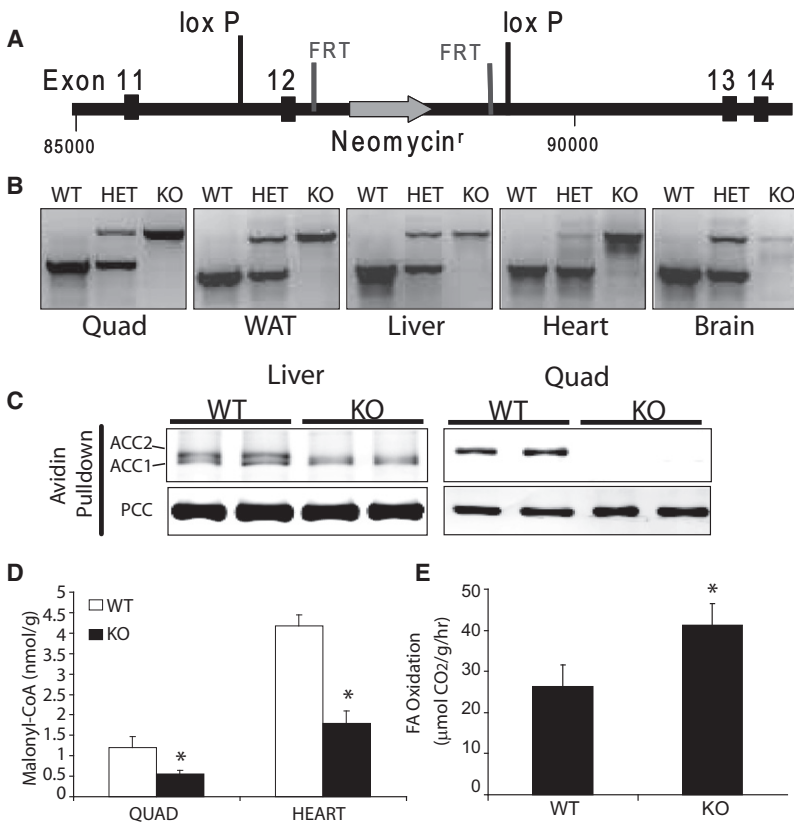


Figure 2. Confirmation of ACC2 Deletion and Phenotype

(A) Exon 12 encodes an essential region of the biotin carboxylase motif and was targeted for deletion. Exon 12 was flanked with loxP sites and subsequently bred with mice expressing Cre recombinase driven by the early acting PGK promoter. Cre-mediated recombination removes exon 12, the Neomycin selection cassette, and causes a frameshift mutation and an early stop codon. The PGK-Cre allele was subsequently bred out. The embryonic stem cells and all crosses were performed with pure C57BL/6 lineage.

(B) PCR confirmation of exon 12 deletion as described in Experimental Procedures.

(C) Protein confirmation of ACC2 deletion by monomeric avidin pulldown (see Experimental Procedures). Membranes were probed with streptavidin 800, and ACC2, ACC1, and propionyl-CoA Carboxylase (PCC) enzymes were identified based on molecular weight.

(D) Malonyl-CoA levels in skeletal and cardiac muscle of WT and ACC2^{-/-} mice.

(E) FAO rates in isolated soleus muscle from WT and ACC2^{-/-} mice. *p < 0.05.

Error bars are displayed as means ± SEM.

interventions ineffective, so there is a growing need for new therapies. The hypothesis that manipulations that enhance fat burning will reduce adiposity has provided novel avenues and new hope for the treatment of obesity. Indeed there is a link between AMPK activation and leanness (Lage et al., 2008; Narkar et al., 2008). Currently, the precise mechanism linking AMPK to leanness is unknown, as AMPK activity has both short and long-term effects. On one hand, AMPK rapidly increases FAO, primarily via its inhibition of ACC. On the other, its prolonged activity regulates many other pathways, such as mitochondrial biogenesis (Bergeron et al., 2001; Winder et al., 2000), uncoupling protein expression (Narkar et al., 2008; Suwa et al., 2003), GLUT4 expression (Winder et al., 2000), and the SIRT1 pathway (Canto et al., 2009). Hence, it is unclear whether AMPK agonists promote leanness via the FAO pathway or an alternate route (Figure 4G).

To address this question, we used pharmacological and genetic manipulations in rodents to increase FAO upstream or downstream of AMPK. We used AICAR to activate AMPK acutely and chronically for 10 days. There was no change in body composition, substrate utilization, or energy expenditure following AICAR treatment at either time point, but there was a clear stimulation of mitochondrial biogenesis in skeletal muscle after 10 days. To test the effects of long-term changes in FAO independently of AMPK, we directly targeted ACC2 in mice. ACC2 inhibition led to reduced intracellular malonyl-CoA levels and a concomitant increase in FAO in skeletal muscle without any change in energy expenditure or adiposity. Rather, in both acute and chronic settings, our data show that increased FAO

is offset by an alteration in the handling of other macronutrients. Our findings are consistent with previous studies using a nonselective ACC1/2 inhibitor in rats. This inhibitor decreased RER over a 3 hr period without altering energy expenditure (Harwood et al., 2003). Second, reduced ACC1/2 expression in rat liver and fat using antisense oligonucleotides was without effect on body weight (Savage et al., 2006). This illustrates that increased FAO is insufficient to promote energy expenditure or weight loss. Rather, the inherent flexibility in the metabolic system compensates for enforced FAO by altering carbohydrate metabolism. Such an effect is consistent with the glucose-FA cycle first proposed by Randle (Randle et al., 1963).

Our data are in contrast to a previous mouse model of ACC2 deficiency that displayed increased energy expenditure (Choi et al., 2007) and a lean phenotype despite hyperphagia (Abu-Elheiga et al., 2001). Although no mechanism for this effect has been described, this mouse model has provided a major incentive for targeting FAO as a treatment for human obesity. Why have we been unable to observe changes in energy expenditure or a lean phenotype in our ACC2^{-/-} mice, despite the fact that they are metabolically similar in almost every other respect to those reported previously (Abu-Elheiga et al., 2001; Choi et al., 2007)? This is unlikely due to a more modest phenotype in our animals because the increase in muscle and whole-body FAO in the ACC2^{-/-} mice described here was more robust than that reported previously (Abu-Elheiga et al., 2001; Choi et al., 2007). There are a number of technical differences between the two studies that may account for this difference. In our studies, we constructed the ACC2 deletion on a genetically pure C57BL/6 mouse background and performed our studies using littermates to avoid founder effects. We also removed the stem cell selection marker from the genome prior to study to avoid potential artifacts, whereas this was not reported in

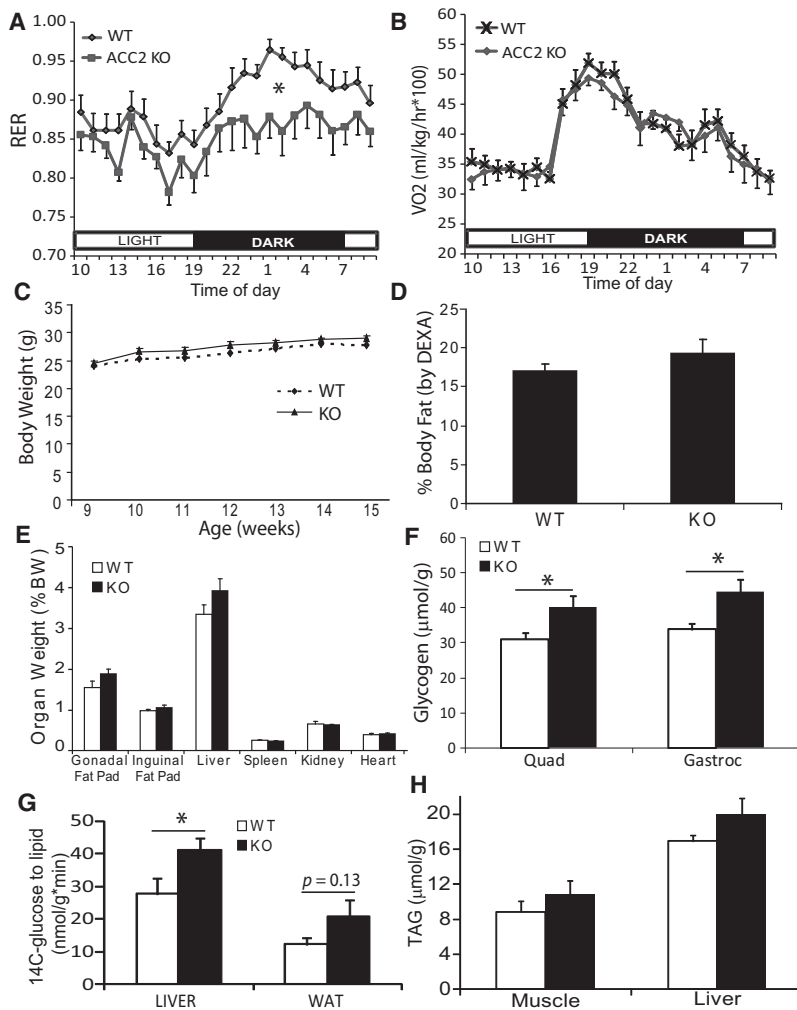


Figure 3. Chronic FAO Increases Glycogen Storage, but Not Energy Expenditure

(A and B) Indirect calorimetry measurements were used to determine RER and VO₂ in male WT and ACC2^{-/-} mice. *p < 0.05 for ACC2^{-/-} versus WT in the dark cycle. (C–E) Body weight, body fat (by DEXA), and organ size (by dissection) were measured in male littermate mice 18–22 weeks of age. n > 5. (F) Glycogen content in hind limb skeletal muscle from male WT and ACC2^{-/-} mice. n = 6. *p < 0.05. (G) 14C-glucose incorporation into lipid in liver and white adipose tissue in WT and ACC2^{-/-} mice following a glucose load (1.5 g/kg). n = 4–7. *p < 0.05. (H) Triacylglycerol content per g of liver tissue in WT and ACC2^{-/-} mice. n = 4. Error bars are displayed as means ± SEM.

Excess adiposity and lipid accumulation in nonadipose tissues are linked to insulin resistance (Savage et al., 2007). However, the effect of increasing FAO on insulin sensitivity is controversial in that some studies indicate that enhancing FAO protects against HFD-induced insulin resistance (Bruce et al., 2009), whereas other studies show that excessive FAO in fact promotes insulin resistance (Koves et al., 2008). In our study, we were unable to observe any protective effect of increased FAO against HFD-induced insulin resistance.

Based on the present study, it is unlikely that increasing lipid oxidation alone is sufficient to cause leanness. In view of the fact that increased FAO was considered one of the major mechanisms of AMPK in fat reduction and leanness, this leaves open the possibility that the adipose-lowering effects of chronic AMPK

activation are mediated via an alternate pathway, such as increased mitochondrial biogenesis or increased expression of uncoupling proteins. Hence, this study supports the traditional view of energy homeostasis, which is that, under normal conditions of thermoneutrality, body mass is principally controlled by the balance between food consumption and ATP hydrolysis and that coercing the animal to metabolize one nutrient in favor of another, as in the case of the ACC2^{-/-} mouse, is compensated for simply by downregulating the use of alternate fuels, with the end result being no change in net energy balance.

the case of the previous studies (Abu-Elheiga et al., 2001), raising the possibility that all tissues in that animal overexpressed an enzyme involved in purine biosynthesis (HPRT). In addition, we targeted an exon closer to the 5' end of the gene at an upstream biotin carboxylase motif, and we could find no evidence for any ACC2 polypeptide expressed in tissues from our animals. Finally, one cannot ignore the fact that, of ~2000 knockout mouse models examined, 30% exhibit a lean phenotype, raising the possibility that either 30% of all genes independently regulate leanness or other processes involved in genetic engineering and selection somehow contribute to leanness (Reed et al., 2008). This, combined with the fact that our ACC2^{-/-} mice phenocopy long-term administration of AICAR in rats, provides strong support for the theory that was advanced by Randle nearly 50 years ago—that energy demand drives energy expenditure and that different substrates compete for entry into the energy utilization pathway in a mutually exclusive manner. Our results provide new evidence to indicate that FAO and energy expenditure are not coupled, and thus the belief that FAO drives leanness is likely incorrect or, at least, an oversimplification. The implications of these findings are considerable, particularly for those investing effort to develop ACC2 inhibitors for the treatment of obesity and type 2 diabetes (Corbett, 2009).

activation are mediated via an alternate pathway, such as increased mitochondrial biogenesis or increased expression of uncoupling proteins. Hence, this study supports the traditional view of energy homeostasis, which is that, under normal conditions of thermoneutrality, body mass is principally controlled by the balance between food consumption and ATP hydrolysis and that coercing the animal to metabolize one nutrient in favor of another, as in the case of the ACC2^{-/-} mouse, is compensated for simply by downregulating the use of alternate fuels, with the end result being no change in net energy balance.

EXPERIMENTAL PROCEDURES

Materials

Antibodies against ACC and phospho-S79 ACC were from Cell Signaling (Beverly, MA). DNP was from Sigma, and AICAR was from Toronto Research Chemicals. Monomeric avidin beads were from Pierce (Rockford, IL). Streptavidin-conjugated IRDye-800 was from Rockland Chemicals (Gilbertsville, PA).

Animals

Food and water were provided *ad libitum* until the date of study, and all animal care was in compliance with the Australian National Health and Medical Research Council guidelines, as well as institutional guidelines at Garvan. The high- and low-fat diets (45% and 8% kcal as fat, respectively) used are

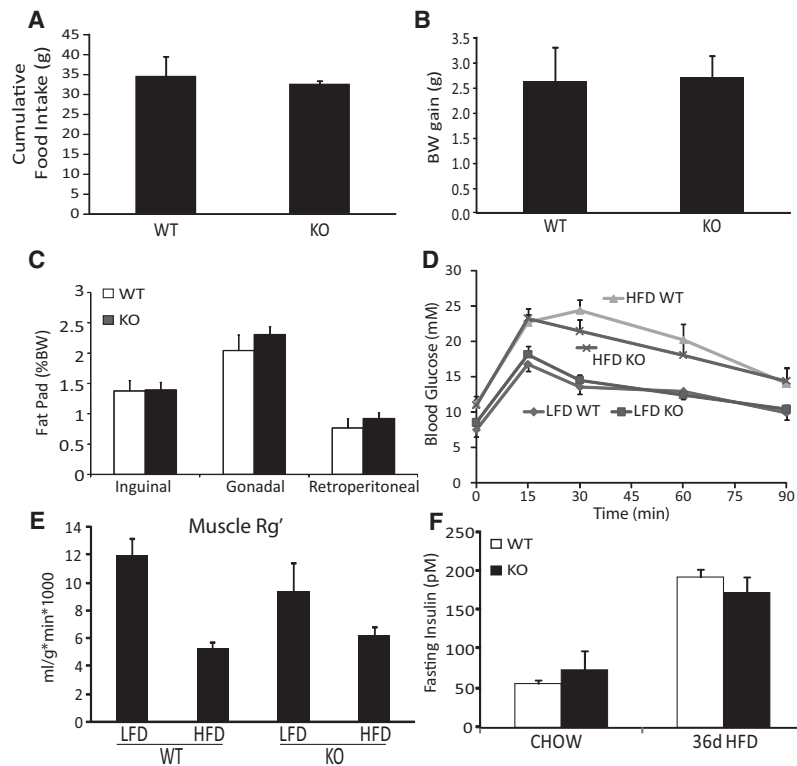


Figure 4. Effects of Chronic FAO on Body Weight Gain and Insulin Sensitivity with 36 Days of High-Fat Feeding

(A–C) Food intake, body weight gain, and fat pad weights were measured over 36 days of high-fat feeding.

(D) Glucose tolerance test of 16-week-old male WT and *ACC2*^{-/-} mice fed a chow diet or high-fat diet. *n* = 5–7 per group.

(E) Skeletal muscle insulin resistance was determined by measuring glucose disposal into skeletal muscle during the glucose tolerance test as described in [Experimental Procedures](#).

(F) Insulin levels were not altered between WT and *ACC2*^{-/-} mice fed either a chow or high-fat diet.

Error bars are displayed as means \pm SEM.

Australia). Clearance of ¹⁴C-glucose (10 μ Ci/animal) into lipid and [³H]-2-DOG (10 μ Ci/animal) into glucose-6-phosphate during the glucose tolerance test were determined using methods described previously (Bruce et al., 2009; Cooney et al., 2004).

Avidin Pulldown

Protein lysates were prepared by homogenizing tissues in NP-40 lysis buffer. 300 μ g protein was incubated with monomeric avidin beads overnight at 4°C. The beads were then washed, and the biotin-containing proteins were eluted with 1 \times Laemmli buffer at 65°C for 5 min. Eluate was run on a 6% SDS-PAGE gel, transferred to PVDF, and probed with streptavidin-conjugated IRDye 800, and biotinylated proteins were detected on a LICOR Odyssey Infrared Scanner.

Enzyme Activity Measurements and Immunoblotting in Muscle

Measurement of the activity of oxidative enzymes and immunoblotting of proteins involved in mitochondrial function and lipid metabolism were conducted as described previously (Bruce et al., 2009; MacArthur et al., 2008).

Respirometry

Oxygen consumption rate (*V*O₂) and respiratory exchange ratio (RER) were measured under a consistent environmental temperature (22°C) using an indirect calorimetry system (Oxymax series, Columbus Instruments, Columbus, OH). For mice, studies were commenced after 2 hr of acclimation to the metabolic chamber using an air flow of 0.6 l/min. *V*O₂ was measured in individual mice at 27 min intervals during a 24 hr period. For the rat studies, the air flow was 1.5 l/min, and measurements were made at 15 min intervals. Animals were placed in the chamber in the late afternoon and on the following morning were dosed with vehicle, AICAR, or DNP at the doses detailed in the figure legends. During the studies, both mice and rats had *ad libitum* access to food and water.

Ex Vivo Muscle Substrate Oxidation

Palmitate and glucose oxidation were determined in muscle strips as described (Bruce et al., 2009; Hoy et al., 2007). In brief, whole soleus from mice or EDL strips from rats were dissected tendon to tendon and placed in a vial containing warmed (30°–34°C), pregassed (95% O₂-5% CO₂ [pH 7.4]), modified Krebs-Henseleit buffer containing 4% FA-free BSA, 5 mM glucose, and 0.5 mM palmitate, giving a palmitate:BSA molar ratio of 1:1. Following a 30 min preincubation period, muscle strips were transferred to vials containing 0.5 μ Ci/ml of [1-¹⁴C] palmitate or 2 μ Ci/ml of [U-¹⁴C] glucose (GE Healthcare Life Sciences, Buckinghamshire, UK) for 60 min. At the completion of this phase, the medium was acidified with 1 M HClO₄, and evolved ¹⁴CO₂ was captured in 1M NaOH.

Blood and Tissue Metabolites

Insulin was measured from whole blood by ELISA (Crystal Chem, Downers Grove, IL). NEFAs were measured calorimetrically (WAKO diagnostics, Osaka

described previously (Bruce et al., 2009). Animals were maintained on a 12/12 light/dark schedule such that lights go out at 7 PM and on at 7 AM.

Generation of *ACC2* Floxed Mice

The *ACC2* gene has 52 exons. We targeted exon 12 because its deletion will destroy the biotin carboxylase motif and will result in a frameshift mutation and an early stop codon. Ozgene Pty Ltd. (Murdoch, Australia) was employed to develop these mice. They designed the *ACC2*-targeting vector FLSniper in three fragments—the 3' arm, the 5' arm, and the loxP arm—by PCR using PGK-Neo-pA-SD-IS as the selection cassette. A BglII site was introduced in the 5' loxP site and was used for targeting confirmation by Southern blotting. The targeting vector was used for homologous recombination by electroporation in Bruce4 embryonic stem (ES) cells. *ACC2*-targeted ES cell clones were identified by PCR and Southern blot hybridization using 5' and 3' flanking probes. Screening with the endogenous probe revealed a 13.8 kb wild-type band, a 7.1 kb targeted band, and a 2.9 kb fragment when the floxed region was deleted by Cre-recombinase (data not shown). The ES cells carrying the correct mutation were injected into BALB/c blastocysts and implanted into foster mothers. Chimeric progeny were bred with C57/BL6 mice to obtain germline founders. These were then bred with heterozygous Cre-deleter mice on a BL/6 background (*ROSA* locus knockin driven by a PGK promoter), and genotyping of progeny was performed by Southern blot or PCR (Figure 2B). The PCR primers for Cre were CCGGTGATGCAACGAGTGAT and ACCAGAGTCATCCTTAGCGCC. Primer sets to differentiate between *ACC2* wild-type, heterozygous, and homozygous knockout were *ACC2* common forward primer AGGATTTGAAGTCAAGTCAAGGCTTGGC, wild-type reverse primer GTACAGAAGCCGTATGCTCCTTCAGTCGGTG, and knockout reverse primer CCTGAGCCGAGTGTGGGACCGTTTAGAC. These three primers were all used in the same PCR reaction and generated products of 750 bp for WT, 1091 bp for KO, and both 750 bp and 1091 bp for HET (Figure 2B). Mice were maintained on a C57BL/6 background and bred with our in-house C57BL/6 line. The Cre allele was bred out for all mice in this study.

Glucose and Insulin Tolerance Testing

Mice were fasted for 6 hr and were then injected intraperitoneally with glucose (1.5 g/kg) or insulin (0.5 U/kg), and blood glucose levels were monitored over time using an Accu-check II glucometer (Roche Diagnostics, Castle Hill,

Japan). TAG and glycogen contents were measured in tissues as described previously (Bruce et al., 2009; Hoy et al., 2007). Malonyl-CoA was measured from rat skeletal muscle 60 min after saline, DNP, or AICAR injection and from wild-type or ACC2KO mice fasted for 12 hr. Malonyl-CoA was measured by LC-MS/MS using a modification of the method described (Minkler et al., 2006). Specific details of the malonyl-CoA assays can be found in the [Supplemental Information](#).

Statistical Analyses

Data are expressed as means \pm standard error. P values were calculated by two-tailed Student's t test or one-way ANOVA with Fisher's PLSD post-hoc test. Statistical significance was set at $p < 0.05$. All results are displayed as means \pm SEM.

SUPPLEMENTAL INFORMATION

Supplemental Information include Supplemental Experimental Procedures and four figures and can be found with this article online at [doi:10.1016/j.cmet.2009.11.008](https://doi.org/10.1016/j.cmet.2009.11.008).

ACKNOWLEDGMENTS

This work was supported by the US National Institute of Health (DK067509 to D.E.J., F32 DK075249 to K.L.H.), National Health and Medical Research Council of Australia (NHMRC) (D.E.J., G.J.C., N.T., E.W.K.), and Diabetes Australia Research Trust and Viertel Trust (K.L.H.). A.J.H. is supported by a University of New South Wales Australian Postgraduate Award. N.T. is supported by a Career Development Award, and E.W.K., G.J.C., and D.E.J. are supported by Research Fellowships from the NHMRC.

Received: April 22, 2009

Revised: September 28, 2009

Accepted: November 23, 2009

Published: January 5, 2010

REFERENCES

- Abu-Elheiga, L., Matzuk, M.M., Abo-Hashema, K.A., and Wakil, S.J. (2001). Continuous fatty acid oxidation and reduced fat storage in mice lacking acetyl-CoA carboxylase 2. *Science* *291*, 2613–2616.
- Bergeron, R., Ren, J.M., Cadman, K.S., Moore, I.K., Perret, P., Pypaert, M., Young, L.H., Semenkovich, C.F., and Shulman, G.I. (2001). Chronic activation of AMP kinase results in NRF-1 activation and mitochondrial biogenesis. *Am. J. Physiol. Endocrinol. Metab.* *281*, E1340–E1346.
- Bruce, C.R., Hoy, A.J., Turner, N., Watt, M.J., Allen, T.L., Carpenter, K., Cooney, G.J., Febbraio, M.A., and Kraegen, E.W. (2009). Overexpression of carnitine palmitoyltransferase-1 in skeletal muscle is sufficient to enhance fatty acid oxidation and improve high-fat diet-induced insulin resistance. *Diabetes* *58*, 550–558.
- Canto, C., Gerhart-Hines, Z., Feige, J.N., Lagouge, M., Noriega, L., Milne, J.C., Elliott, P.J., Puigserver, P., and Auwerx, J. (2009). AMPK regulates energy expenditure by modulating NAD⁺ metabolism and SIRT1 activity. *Nature* *458*, 1056–1060.
- Choi, C.S., Savage, D.B., Abu-Elheiga, L., Liu, Z.X., Kim, S., Kulkarni, A., Distefano, A., Hwang, Y.J., Reznick, R.M., Codella, R., et al. (2007). Continuous fat oxidation in acetyl-CoA carboxylase 2 knockout mice increases total energy expenditure, reduces fat mass, and improves insulin sensitivity. *Proc. Natl. Acad. Sci. USA* *104*, 16480–16485.
- Cooney, G.J., Lyons, R.J., Crew, A.J., Jensen, T.E., Molero, J.C., Mitchell, C.J., Biden, T.J., Ormandy, C.J., James, D.E., and Daly, R.J. (2004). Improved glucose homeostasis and enhanced insulin signalling in Grb14-deficient mice. *EMBO J.* *23*, 582–593.
- Corbett, J.W. (2009). Review of recent acetyl-CoA carboxylase inhibitor patents: mid-2007–2008. *Expert. Opin. Ther. Pat.* *19*, 943–956.
- Harwood, H.J., Jr., Petras, S.F., Shelly, L.D., Zaccaro, L.M., Perry, D.A., Makowski, M.R., Hargrove, D.M., Martin, K.A., Tracey, W.R., Chapman, J.G., et al. (2003). Isozyme-nonselective N-substituted bipiperidylcarboxamide acetyl-CoA carboxylase inhibitors reduce tissue malonyl-CoA concentrations, inhibit fatty acid synthesis, and increase fatty acid oxidation in cultured cells and in experimental animals. *J. Biol. Chem.* *278*, 37099–37111.
- Hoy, A.J., Bruce, C.R., Cederberg, A., Turner, N., James, D.E., Cooney, G.J., and Kraegen, E.W. (2007). Glucose infusion causes insulin resistance in skeletal muscle of rats without changes in Akt and AS160 phosphorylation. *Am. J. Physiol. Endocrinol. Metab.* *293*, E1358–E1364.
- Jäger, S., Handschin, C., St-Pierre, J., and Spiegelman, B.M. (2007). AMP-activated protein kinase (AMPK) action in skeletal muscle via direct phosphorylation of PGC-1 α . *Proc. Natl. Acad. Sci. USA* *104*, 12017–12022.
- Kelley, D.E., He, J., Menshikova, E.V., and Ritov, V.B. (2002). Dysfunction of mitochondria in human skeletal muscle in type 2 diabetes. *Diabetes* *51*, 2944–2950.
- Koves, T.R., Ussher, J.R., Noland, R.C., Slentz, D., Mosedale, M., Ilkayeva, O., Bain, J., Stevens, R., Dyck, J.R., Newgard, C.B., et al. (2008). Mitochondrial overload and incomplete fatty acid oxidation contribute to skeletal muscle insulin resistance. *Cell Metab.* *7*, 45–56.
- Lage, R., Diéguez, C., Vidal-Puig, A., and López, M. (2008). AMPK: a metabolic gauge regulating whole-body energy homeostasis. *Trends Mol. Med.* *14*, 539–549.
- MacArthur, D.G., Seto, J.T., Chan, S., Quinlan, K.G., Raftery, J.M., Turner, N., Nicholson, M.D., Kee, A.J., Hardeman, E.C., Gunning, P.W., et al. (2008). An Actn3 knockout mouse provides mechanistic insights into the association between alpha-actinin-3 deficiency and human athletic performance. *Hum. Mol. Genet.* *17*, 1076–1086.
- Minkler, P.E., Kerner, J., Kasumov, T., Parland, W., and Hoppel, C.L. (2006). Quantification of malonyl-coenzyme A in tissue specimens by high-performance liquid chromatography/mass spectrometry. *Anal. Biochem.* *352*, 24–32.
- Narkar, V.A., Downes, M., Yu, R.T., Embler, E., Wang, Y.X., Banayo, E., Mihaylova, M.M., Nelson, M.C., Zou, Y., Juguillon, H., et al. (2008). AMPK and PPAR- δ agonists are exercise mimetics. *Cell* *134*, 405–415.
- Petersen, K.F., Befroy, D., Dufour, S., Dziura, J., Ariyan, C., Rothman, D.L., DiPietro, L., Cline, G.W., and Shulman, G.I. (2003). Mitochondrial dysfunction in the elderly: possible role in insulin resistance. *Science* *300*, 1140–1142.
- Randle, P.J., Garland, P.B., Hales, C.N., and Newsholme, E.A. (1963). The glucose fatty-acid cycle. Its role in insulin sensitivity and the metabolic disturbances of diabetes mellitus. *Lancet* *1*, 785–789.
- Reed, D.R., Lawler, M.P., and Tordoff, M.G. (2008). Reduced body weight is a common effect of gene knockout in mice. *BMC Genet.* *9*, 4.
- Savage, D.B., Choi, C.S., Samuel, V.T., Liu, Z.X., Zhang, D., Wang, A., Zhang, X.M., Cline, G.W., Yu, X.X., Geisler, J.G., et al. (2006). Reversal of diet-induced hepatic steatosis and hepatic insulin resistance by antisense oligonucleotide inhibitors of acetyl-CoA carboxylases 1 and 2. *J. Clin. Invest.* *116*, 817–824.
- Savage, D.B., Petersen, K.F., and Shulman, G.I. (2007). Disordered lipid metabolism and the pathogenesis of insulin resistance. *Physiol. Rev.* *87*, 507–520.
- Suwa, M., Nakano, H., and Kumagai, S. (2003). Effects of chronic AICAR treatment on fiber composition, enzyme activity, UCP3, and PGC-1 in rat muscles. *J. Appl. Physiol.* *95*, 960–968.
- Winder, W.W., Holmes, B.F., Rubink, D.S., Jensen, E.B., Chen, M., and Holloszy, J.O. (2000). Activation of AMP-activated protein kinase increases mitochondrial enzymes in skeletal muscle. *J. Appl. Physiol.* *88*, 2219–2226.